A. Baz
*Mechanical Engineering Department
The Catholic University of America
Washington, DC 20064*

Continuous Sliding Mode Control of Flow-Induced Vibrations

Vortex-induced vibrations of flexible circular cylinders and galloping oscillations of square prisms are controlled using a robust continuous sliding mode (CSM) controller. The ability of the CSM controller in rejecting the flow-induced disturbances and accommodating parameter uncertainties is numerically demonstrated. In the present study, emphasis is placed on the development of theoretical models that describe the interaction between the flexible structures, the flow-induced excitation, and the CSM controller. In our development, the vortex-induced vibrations are based on the lift-oscillator model of Hartlen and Currie and the galloping phenomenon is described using Parkinson and Smith's model. The effectiveness of the CSM controller in suppressing the flow-induced vibrations of cylinders and square prisms is evaluated at various flow conditions and levels of structural uncertainties. The effect of the design parameters of the CSM controller on its performance is also investigated. The results obtained in the study suggest the potential of the robust control strategy presented as an important tool for rejecting undesirable and unmeasurable disturbances acting on critical structures that have considerably large parameter uncertainties.

INTRODUCTION

Considerable emphasis has been placed recently on the development of active control systems for damping out flow-induced vibrations arising from periodic shedding of Von Karman vortices from the flexible cylindrical structures or from the galloping/flutter instabilities of structures with noncircular cross sections. Such active control systems employ a wide range of control strategies including: simple ON–OFF control (Klein and Healey, 1985), optimal linear quadratic regulator (Soong and Skinner, 1981), and optimal linear quadratic tracker (Abdel–Rohman, 1984). More recently, a direct velocity feedback controller was used by Baz and Ro (1991) to control a single vibration mode with a single pair of collocated sensor/actuator. Also, Baz and Kim (1993) utilized a modified independent modal space method to control vortex-induced vibrations of circular cylinders using single or multiple noncollocated sensors and actuators.

Venkatraman and Narayanan (1993) presented a radically different control approach where a disturbance counteracting control law is utilized to control vortex-induced vibrations of circular cylinders and galloping of square prisms. The control law relies on a disturbance observer to estimate the magnitude of the flow-induced excitation, which are assumed to be periodic. Poh and Baz (1994) used an adaptive least mean square (LMS) method to control the vibration of a flexi-

Received Nov. 14, 1994; Accepted April 27, 1995.

Shock and Vibration, Vol. 2, No. 5, pp. 365–372 (1995)

CCC 1070-9622/95/050365-08

ble cylinder by rejecting the periodic vortex-induced disturbance. In that study, the control action was generated without the need for a disturbance observer. However, a hot wire anemometer placed in the wake of the cylinder was used to generate a reference signal that indicates the vortex shedding excitation. The anemometer was used in addition to the other sensors needed for monitoring the structural vibrations.

In the present study, a robust continuous sliding mode (CSM) method is introduced that does not require the use of a disturbance observer as described by Venkatraman and Narayanan (1993) or of a disturbance reference sensor as reported by Poh and Baz (1994). Moreover, the method presented does not require the flow-induced excitation to be periodic in nature as assumed by Venkatraman and Narayanan (1993). It requires only a very rough estimate of an upper bound on the *total* flow-induced excitation. In that regard, the CSM method does not require any distinction between time-dependent and state-dependent excitations as carried out by Venkatraman and Narayanan (1993).

It is also important to note that the robust CSM method proposed here is not only capable of rejecting the unmeasurable flow-induced disturbances, but also capable of accommodating bounded uncertainties of the structural parameters. In this manner, the CSM method presents a much simpler yet more powerful alternative to the classical control methods, disturbance counteracting law and the LMS algorithm.

The effectiveness of the CSM controller in suppressing vortex-induced vibrations of cylinders and galloping of square prisms is addressed theoretically in this article. Reviews of Hartlen and Currie's lift-oscillator model for vortex-induced vibrations (1970) and Parkinson and Smith's model for galloping oscillations (1964) are given; the concept of the Sliding Mode Controller (SMC) is described; the effectiveness of the SMC in suppressing the flow-induced vibrations of cylinders and square prisms is demonstrated; and a summary of the main results is given.

FLOW-INDUCED VIBRATION MODELS

The dynamical models describing the vortex-induced vibrations of flexible cylinders and the galloping oscillations of square prisms are presented in this section.

Vortex-Induced Vibrations

Periodic shedding of vortices from the surfaces of cylinders generates periodic lift forces that tend to excite these cylinders in the transverse direction as shown in Fig. 1. The induced oscillations, in turn, interact with the vortices in such a way that amplifies the lift forces.

The resulting fluid–structure interaction can be described by Hartlen and Currie's model (1970) as follows: cylinder:

$$\ddot{x} + 2\zeta\dot{x} + x = a\omega_0^2 c_L = F_v; \tag{1}$$

fluid:

$$\ddot{c}_L - \alpha\omega_o\dot{c}_L + \gamma/\omega_0\dot{c}_L^3 + \omega_0^2 c_L = b\dot{x}. \tag{2}$$

Equation (1) defines the dynamics of the cylinder, represented by its motion x in the transverse direction, as excited by the fluid lift forces F_v.

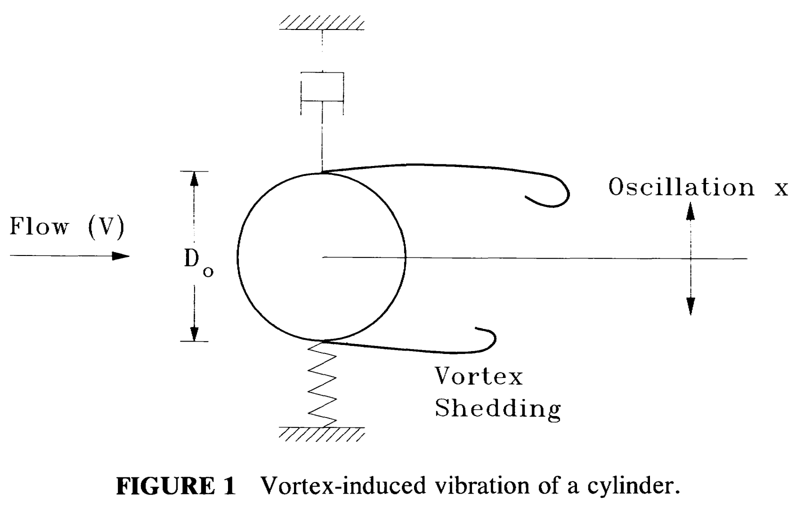

FIGURE 1 Vortex-induced vibration of a cylinder.

Equation (2) represents the lift-oscillator model that simulates the effect of the periodic shedding of the vortices on the lift coefficient c_L. The fluid–structure interactions are evident from the coupling terms appearing on the right-hand sides (rhs) of Eqs. (1) and (2). Note that such interaction is of the self-excited and self-limited type.

In Eqs. (1) and (2), the overdots denote derivative with respect to dimensionless time ($\omega_n t$) and x is the displacement of the cylinder normalized with respect to cylinder diameter D_c. Also, ω_0 is the reduced flow velocity ($=\omega_s/\omega_n$), ω_n is natural frequency of cylinder, and ω_s is shedding frequency. The damping ratio is ζ, and the mass ratio parameter $a = \rho D_c^2 L/8\pi^2 S^2 M$ with ρ, L, S, and M as the fluid density, cylinder length, Strouhal number, and cylinder mass. The parameters α and γ are related to the limit cycle lift coefficient c_{LO} by $c_{LO} = [4\alpha/3\gamma]^{1/2}$ and b is a chosen amplification factor.

Galloping Vibrations of Square Prisms

Galloping represents low frequency and high amplitude oscillations resulting from the flow-induced instabilities of structures with noncircular sections. The associated fluid-dynamic forces vary nonlinearly with the transverse velocity of the structures resulting in amplitudes of oscillations that increase with increasing flow velocities. For square prisms (shown schematically in Fig. 2), galloping occurs spontaneously because these prisms are unstable starting from rest (Parkinson and Smith, 1964).

The dynamics of square prisms undergoing galloping oscillations are simulated by the dimensionless model of Parkinson and Smith (1964) as follows: prism:

$$\ddot{y} + 2\zeta\dot{y} + y = 1/2 C_{Fy} m U^2 = F_g \tag{3}$$

fluid:

$$C_{Fy} = \overline{A}(\dot{y}/U) - \overline{B}(\dot{y}/U)^3 + \overline{C}(\dot{y}/U)^5 - \overline{D}(\dot{y}/U)^7. \tag{4}$$

Equation (3) defines the dynamics of the square prism, described by its motion y in the transverse direction, as excited by the fluid dynamic forces F_g. Equation (4) defines the coefficient of the fluid forces as influenced by the angle of attack β given by $\beta = \tan^{-1}(\dot{y}\ U)$. Note that the fluid–structure interactions are evident from the coupling terms appearing on the rhs of Eqs. (3) and (4). Such interaction is also of the self-excited and self-limited type.

In equations (3) and (4), the dots denote derivative with respect to dimensionless time ($\omega_n t$) and y is displacement of the prism normalized with respect to the length h of its side. Also, U is the reduced flow velocity ($=V/\omega_n h$), V is the flow velocity, and ω_n is natural frequency of the prism $= \sqrt{K_s/M}$ with K_s and M denoting the stiffness and mass of the prism. The damping ratio is ζ, and the mass ratio parameter $m = \rho h^2 L/M$ with ρ and L the fluid density and prism length. The parameters $\overline{A}$, $\overline{B}$, $\overline{C}$, and $\overline{D}$ are suitably chosen to closely fit the experimental coefficient of the fluid forces.

State-Space Representation

The open-loop dynamics of cylinders undergoing vortex-induced vibrations, as given by Eq. (1), and square prisms experiencing galloping oscillations, as described by Eq. (3), can be represented in a unified manner by the following state-space representation:

$$\dot{X} = AX + Gd \tag{5}$$

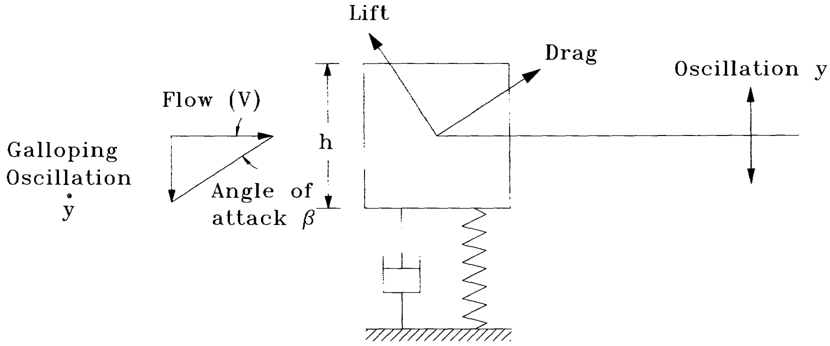

FIGURE 2 Galloping of a square prism.

where X and d denote the state variables vector and the flow-induced disturbance given by: vortex-induced vibrations:

$$X = [x \quad \dot{x}]^T \quad \text{and} \quad d = F_v \tag{6}$$

and galloping vibrations:

$$X = [y \quad \dot{y}]^T \quad \text{and} \quad d = F_g. \tag{7}$$

Also, A and G denote the system and input disturbance matrices given by:

$$A = \begin{bmatrix} 0 & 1 \\ -1 & -2\zeta \end{bmatrix} \quad \text{and} \quad G = [0 \quad 1]^T. \tag{8}$$

In the unified state-space representation of the vortex-induced vibrations and the galloping oscillations, Eq. (5), no distinction has been made between the flow-induced disturbances that are time dependent (e.g. F_v) or state dependent (e.g. F_g).

The open-loop equation, Eq. (5), is augmented by the CSM control action to form the closed-loop equation in order to study the capabilities of the CSM method in attenuating different types of flow-induced vibrations.

CSM CONTROL METHOD

General

The CSM controller is based on the variable structure-sliding mode (VSSM) control method developed by Utkin (1977, 1992). In this method the controller is allowed to change its structure along a carefully selected switching hyperplane in a manner similar to the minimum time bang–bang controller (Lewis, 1986). The reward for this switching is to combine useful properties of the individual control structures. The controller can then force the trajectory of the structure (i.e., the cylinders or the prisms) to follow the switching hyperplane, which is called the sliding surface. Itkis (1976) showed that the VSSM controller is also insensitive to parameter variation and to disturbances.

The VSSM controller suffers, however, from the serious problem of *chattering,* which is attributed to its switching nature. Several schemes have been proposed to alleviate this problem but they significantly contribute to the complexity of the development and implementation of the controller (Hung, 1993).

Zhou and Fisher (1992) introduced the CSM controller to completely eliminate the chattering problem and maintain the stable attributes of the sliding mode controller. This CSM controller is utilized in this study to control vortex-induced vibrations of cylinders and galloping of square prisms. In the development of the CSM controller, no knowledge of the flow characteristics is needed except for a *rough* estimate of the maximum value of the flow force.

The CSM Controller

The open-loop equation, (5), is augmented with the CSM controller to yield the following closed-loop equation:

$$\dot{X} = AX + Bu + Gd \tag{9}$$

where B is control input matrix, $(=[0 \quad 1]^T)$, and u is control force, given by

$$u = -KX - u_d \tag{10}$$

where K is controller gain given by:

$$K = \overline{\alpha} + \delta p^T B p^T \tag{11}$$

$$\overline{\alpha} = (p^T B)^{-1} (p^T A) \tag{12}$$

where δ is a positive number and u_d is a disturbance rejection control action given by:

$$u_d = (([\overline{\beta} + \delta_d]/\lambda) p^T B p^T) X \tag{13}$$

with λ, δ_d positive numbers and

$$\overline{\beta} = \sup[(p^T B)^{-1} (p^T G) d]. \tag{14}$$

Equation (13) shows that the disturbance rejection control action is put in a full state feedback form and Eq. (14) defines the maximum limit of the expected flow-induced disturbance.

In the above equation p^T denotes the slope of the sliding plane:

$$\sigma = p^T X \tag{15}$$

on which the performance of the vibrating structure (i.e., cylinder or prism) will converge and move to reach the origin of the phase plane indicating that the structure has become completely stationary. The coefficient of p^T can be selected by classical pole placement methods or by optimal control strategies.

Stability with Continuous Sliding Mode Controller

Based on the interaction of the dynamics of the flexible structure, the flow-induced excitation and the CSM controller, given by Eqs. (9)–(14), the stability of the total system can be established using Lyapunov stability criterion.

Defining a positive definite Lyapunov function $V_L = \frac{1}{2}\sigma^2$, it can be easily shown that its time derivative $\dot{V}_L$ is

$$\dot{V}_L = \sigma\dot{\sigma} = -\delta(\sigma p^T B)^2 - (\sigma p^T B)\{([\bar{\beta} + \delta_d]/\lambda)p^T B\sigma - \beta\}. \quad (16)$$

The first term on the rhs is negative definite and the second term can be made negative definite by selecting λ small enough such that $[\bar{\beta} + \delta_d]/\lambda)p^T B\sigma$ becomes $\gg\beta$. Under these conditions $\dot{V}$ becomes negative definite and the controller will be able to stabilize the system and reject the flow-induced disturbance.

PERFORMANCE OF CSM CONTROLLER

The effectiveness of the CSM method in damping out flow-induced vibrations of cylinders and square prisms is evaluated at different flow speeds, parameter uncertainty, and controller design parameters. The merits, limitations, and abilities of the CSM controller to reject *unmeasurable* disturbances acting on flexible structures with uncertain parameters is demonstrated.

Control of Vortex-Induced Vibrations

The parameters of the flexible cylinder are selected to be the same as that of Hartlen and Currie's (1970) as indicated in Table 1.

The controller parameters are selected to be as follows:

$$p^T = [1 \quad 2], \quad \bar{\beta} = 1, \quad \delta = 2, \quad \delta_d = 2, \quad \lambda = 0.1.$$

The initial conditions are selected as follows:

$$c_L(0) = 0.2, \quad \dot{c}_L(0) = 0.0, \quad x(0) = 0.2, \quad \dot{x}(0) = 0.0.$$

The combined equations of the cylinder and CSM controller are integrated using a step size of 0.0015 when the cylinder is subjected to sinusoidal fluid-induced excitations at $\omega_0 = 1$.

Figure 3(a) shows the uncontrolled response of x and the corresponding lift coefficient c_L. Limit cycle amplitudes of oscillation of the cylinder of 0.2 are attained while the lift coefficient reaches steady-state amplitude of 0.56.

Activating the controller results in perfect rejection of the flow-induced disturbance after a dimensionless time of 2 as can be seen from Fig. 3(b). Furthermore, the lift coefficient reaches a much lower limit cycle amplitude that is the same as that of a rigid cylinder. The amplification of the lift coefficient, which typically results from the synchronous vibration of the cylinder with the vortex shedding, is eliminated completely.

Figure 4(a,b) show plots of the trajectories of the motion of the uncontrolled and controlled cylinder on the phase plane ($X - \dot{X}$). It is evident that the uncontrolled cylinder attains a limit cycle whereas the controlled cylinder moves directly toward the sliding line and slides along it to reach the origin of the phase plane.

Figure 5 shows that the same excellent performance is maintained even though the natural frequency of the cylinder is reduced to half its value. Therefore, no degradation in the CSM controller performance is observed in the presence of 50% uncertainty in the structural parameters of the cylinder.

Control of Galloping

The parameters of the square prism considered in this study, are selected to be the same as that of Parkinson and Smith's (1964) as indicated in Table 2. The controller parameters are selected to be as follows:

$$p^T = [1 \quad 2], \quad \bar{\beta} = 1, \quad \delta = 2, \quad \delta_d = 2, \quad \lambda = 0.1.$$

Table 1. Parameters of Vibrating Cylinder

Parameter	a	b	α	γ	ζ	ω_0
Value	0.002	0.4	0.02	0.667	0.0015	1.0

Adapted from Hartlen and Currie (1970).

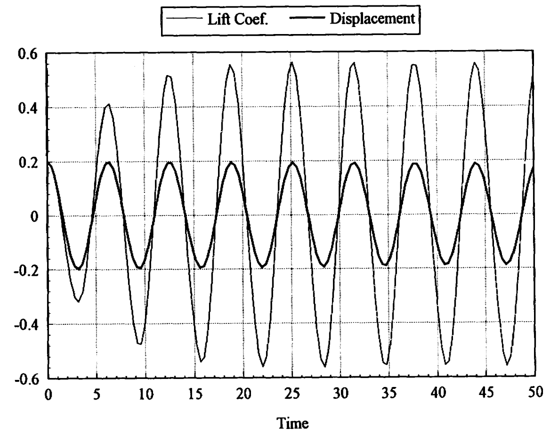

FIGURE 3(a) Time response of x and c_L of the uncontrolled cylinder.

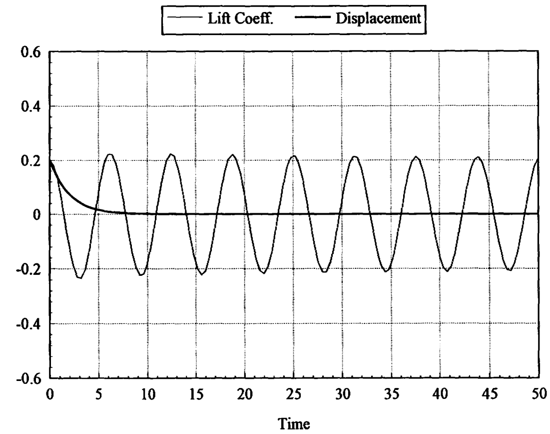

FIGURE 3(b) Time response of x and c_L of the controlled cylinder.

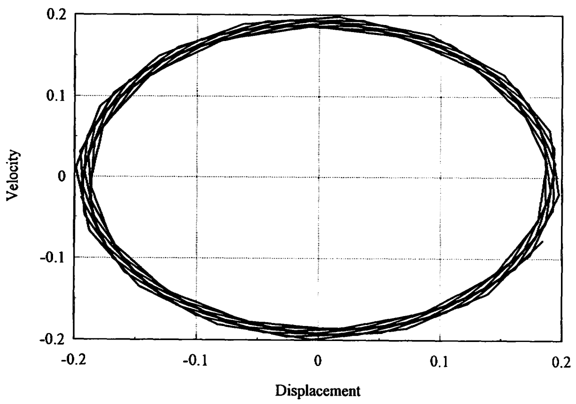

FIGURE 4(a) Trajectory of the uncontrolled cylinder in the phase plane, $\omega_0 = 1$, $x(0) = 0.2$.

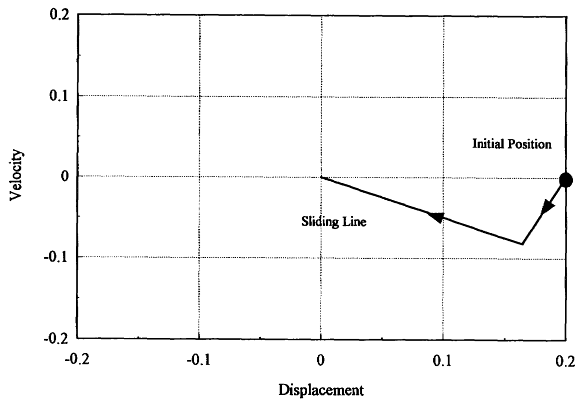

FIGURE 4(b) Trajectory of the controlled cylinder in the phase plane showing the sliding line, $\omega_0 = 1$, $x(0) = 0.2$.

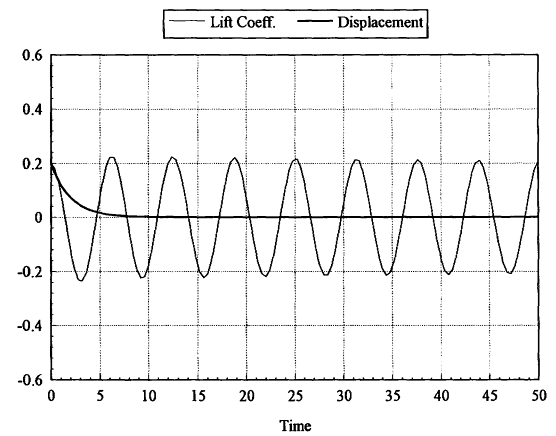

FIGURE 5 Time response of X and c_L of the controlled cylinder with 50% uncertainity in natural frequency, $\omega_0 = 2$, $x(0) = 0.2$.

The initial conditions are selected as follows:

$$y(0) = 0.5, \quad \dot{y}(0) = 0.0, \quad U = 2.$$

Figure 6(a) shows the uncontrolled time response x of the prism. Limit cycle amplitudes of oscillation of the prism of 0.55 are attained.

Activating the controller results in perfect rejection of the flow-induced disturbance after a dimensionless time of about 3 as can be seen from Fig. 6(b).

Figure 7(a,b) show plots of the state trajectories of the uncontrolled and controlled prism on the phase plane $(X - \dot{X})$. Note that the uncontrolled prism reaches a state of limit cycle, and the controlled prism slides along the sliding line to reach the origin of the phase plane.

Table 2. Parameters of Vibrating Square Prism

Parameter	$\bar{A}$	$\bar{B}$	$\bar{C}$	$\bar{D}$	ζ	m
Value	2.69	168	6270	59900	0.00196	0.00043

Adapted from Parkinson and Smith (1964).

Figure 8 shows that reducing the natural frequency of the prism by 50% did not result in any degradation of the CSM controller performance. Hence, the CSM controller is capable of accommodating large uncertainty in the structural parameters of the prism.

CONCLUSIONS

This article presented an application of the robust control theory to the problem of active control of vortex-induced vibrations of flexible circular cylinders and galloping oscillations of square prisms. A continuous SMC was presented and shown to be capable of rejecting the persistent and unmeasurable flow-induced disturbances. The controller was also shown to behave without any performance degradation in the presence of large uncertainty in the structural parameters of the vibrating structures.

The CSM method is simple to implement because it does not require the use of disturbance observers or reference sensors. It does not also assume that the flow-induced excitation are periodic in nature, but it requires only a very rough

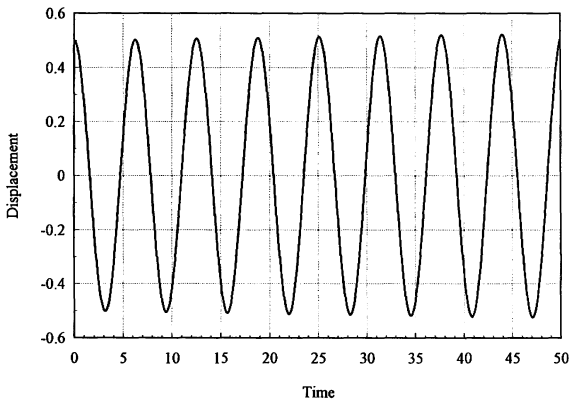

FIGURE 6(a) Time response of y of the uncontrolled prism, $y(0) = 0.5$, $U = 2$.

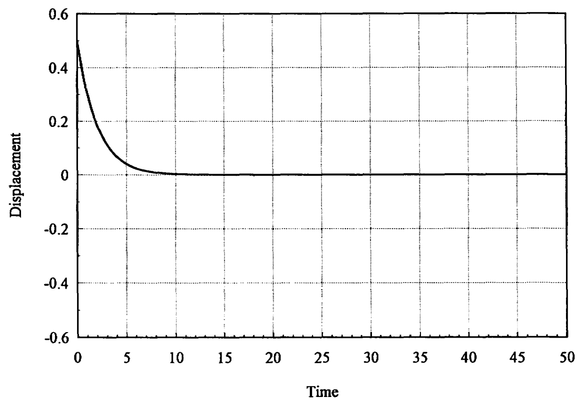

FIGURE 6(b) Time response of y of the controlled prism, $y(0) = 0.5$, $U = 2$.

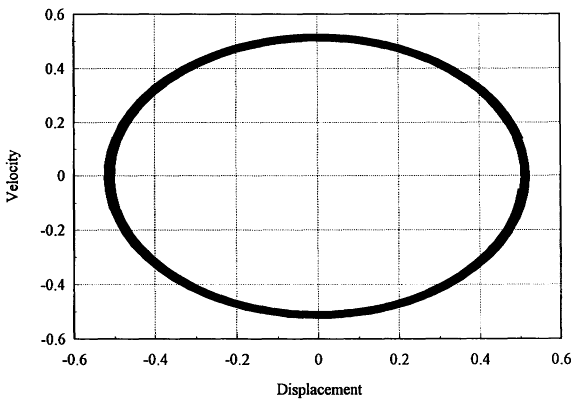

FIGURE 7(a) Trajectory of the uncontrolled prism in the phase plane $y(0) = 0.5$, $U = 2$.

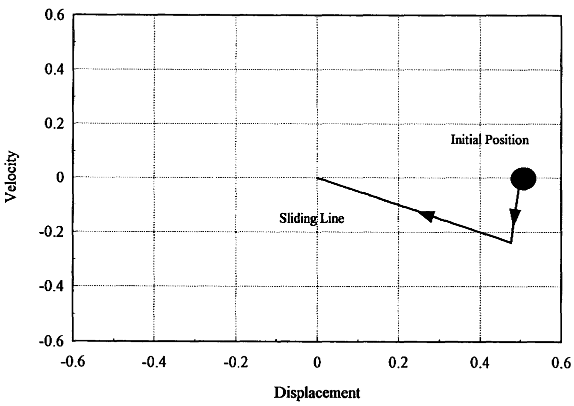

FIGURE 7(b) Trajectory of the controlled prism in the phase plane showing the sliding line, $y(0) = 0.5$, $U = 2$.

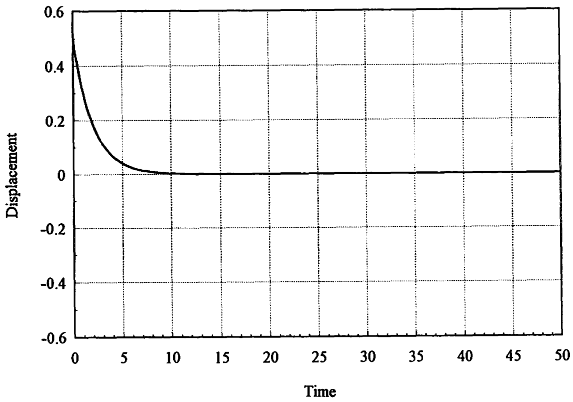

FIGURE 8 Time response of y of the controlled prism with 50% uncertainty in natural frequency, $y(0) = 0.5$, $U = 1$.

estimate of an upper bound on the total flow-induced excitation. Furthermore, the CSM method does not require any distinction between time-dependent and state-dependent excitations.

Such excellent features of the CSM control strategy emphasize its potential in controlling more complex structures that are subject to more complex excitations.

REFERENCES

Abdel-Rohman, M., 1984, "Optimal Control of Tall Buildings by Appendages," *ASCE, Journal of Structural Engineering,* Vol. 110, pp. 937–947.

Baz, A., and Ro, J., 1991, "Active Control of Flow-Induced Vibrations of a Flexible Cylinder Using Direct Velocity Feedback," *Journal of Sound and Vibration,* Vol. 146, pp. 33–45.

Baz, A., and Kim, M., 1993, "Active Modal Control of Vortex-Induced Vibrations of A Flexible Cylinder," *Journal of Sound and Vibration,* Vol. 165, pp. 69–84.

Hartlen, R., and Currie, I., 1970, "Lift-Oscillator Model of Vortex-Induced Vibrations," *ASCE, Journal of Engineering Mechanics,* Vol. 98, pp. 577–591.

Hung, J. Y., 1993, "Variable Structure Control: A Survey," *IEEE Transactions on Industrial Electronics,* Vol. 40, pp. 2–22.

Itkis, U., 1976, *Control Systems of Variable Structure,* A Halsted Press Book, Wiley, New York.

Klein, R., and Healey, M. D., 1985, "Semi-Active Control of Wind-Induced Oscillations in Structures," in H. H. Leipholz, Ed. *Structural Control,* Martinus Nijhoff Publishers, Dordrecht, The Netherlands, pp. 354–369.

Lewis, F., 1986, *Optimal Control,* Wiley, New York.

Parkinson, G., and Smith, J., 1964, "The Square Prism as an Aeroelastic Non-Linear Oscillator," *Quarterly Journal of Mechanics and Applied Math.,* Vol. 17, pp. 225–239.

Poh, S., and Baz, A., 1994, "Active Control of Vortex-Induced Vibration Using an Adaptive Least Mean Square Controller," to appear.

Soong, T. T., and Skinner, G. T., 1981, "Experimental Study of Active Structural Control," *ASCE, Journal of Engineering Mechanics,* Vol. 107, pp. 1057–1067.

Utkin, V., 1977, "Variable Structure Systems with Sliding Modes: Survey Paper," *IEEE Trans on Automatic Controls,* AC-22, pp. 212–222.

Utkin, V., 1992, *Sliding Modes in Control Optimization,* Springer–Verlag, Berlin.

Venkatraman, K., and Narayanan, S., 1993, "Active Control of Flow-Induced Vibration," *Journal of Sound and Vibration,* Vol. 162, pp. 43–55.

Zhou, F., and Fisher, D., 1992, "Continuous Sliding Mode Control," *International Journal of Control.* Vol. 55, pp. 313–327.